

Supplementary Materials for

Discovering the dual degradation pathway of emerald green in oil paints: The effects of light and humidity

Sara Carboni Marri *et al.*

Corresponding author: Letizia Monico, letizia.monico@cnr.it; Aldo Romani, aldo.romani@unipg.it

Sci. Adv. **11**, eady1807 (2025)
DOI: 10.1126/sciadv.ady1807

This PDF file includes:

Supplementary Text
Figs. S1 to S10
Tables S1 and S2

S1. MA-XRPD mapping and XRPD measurements

MA-XRPD mapping

In-situ macro-XRPD measurements were performed using a mobile scanner developed in the AXIS group at the University of Antwerp (69). The device employs an X-ray micro tube as source (50 W, I μ S-Cu, Incoatec GmbH, Germany), generating a monochromatic and focused X-ray beam (Cu-K α ; 8.04 keV) with a photon flux of $3 \cdot 10^8$ ph/s. A 10° angle was chosen between the painting surface and the source due to geometrical constraints. This implies a beam elongation of about 0.8 mm horizontally and 0.2 mm vertically when it hits the sample. The resulting 2D diffraction pattern was recorded using a PILATUS 200K area detector (Dectris Ltd., Switzerland). The instrument is mounted on a motorized XYZ platform. A laser distance sensor (Baumer Hold., Switzerland) automatically adjusted the distance between the artwork and the scanner at each measurement point. The analyzed area (Fig. S1) measured 170×160 mm² (h×v) and was scanned with a step size of 1.2×1.2 mm² and an exposure time of 10 s/pt. The software package XRDUA (68) was used to identify crystalline phases and extract crystalline-specific distributions from the 2D diffraction patterns obtained via XRPD.

XRPD measurements

Structural analysis of emerald green powders and the paint tube was performed using a laboratory D8 Advance diffractometer in Bragg-Brentano geometry. The diffractometer is equipped with a Lynxeye XE-T fast detector (Bruker AXS, Karlsruhe, Germany) and employs Cu-K α radiation operating at 40 kV and 40 mA. Data were collected using a 0.0160° 2 θ step size and a 1 s exposure time. Crystalline phases were identified by a search and match procedure with Bruker Diffract-Eva program (version 2020) and the COD database. The XRPD patterns were processed by Rietveld refinement employing the GSAS-EXPGUI and GSAS-II software packages (70, 71). The refinement procedure included adjusting parameters for the scale factor, background, unit cell, and peak profile parameters. Where possible, microstructural information, such as the average size of coherent diffraction domains and microstrain, was extracted from the peak profile parameters. The refinement also yielded quantitative values of the crystalline phases weight fractions.

S2. XPRD investigations of *The Intrigue*

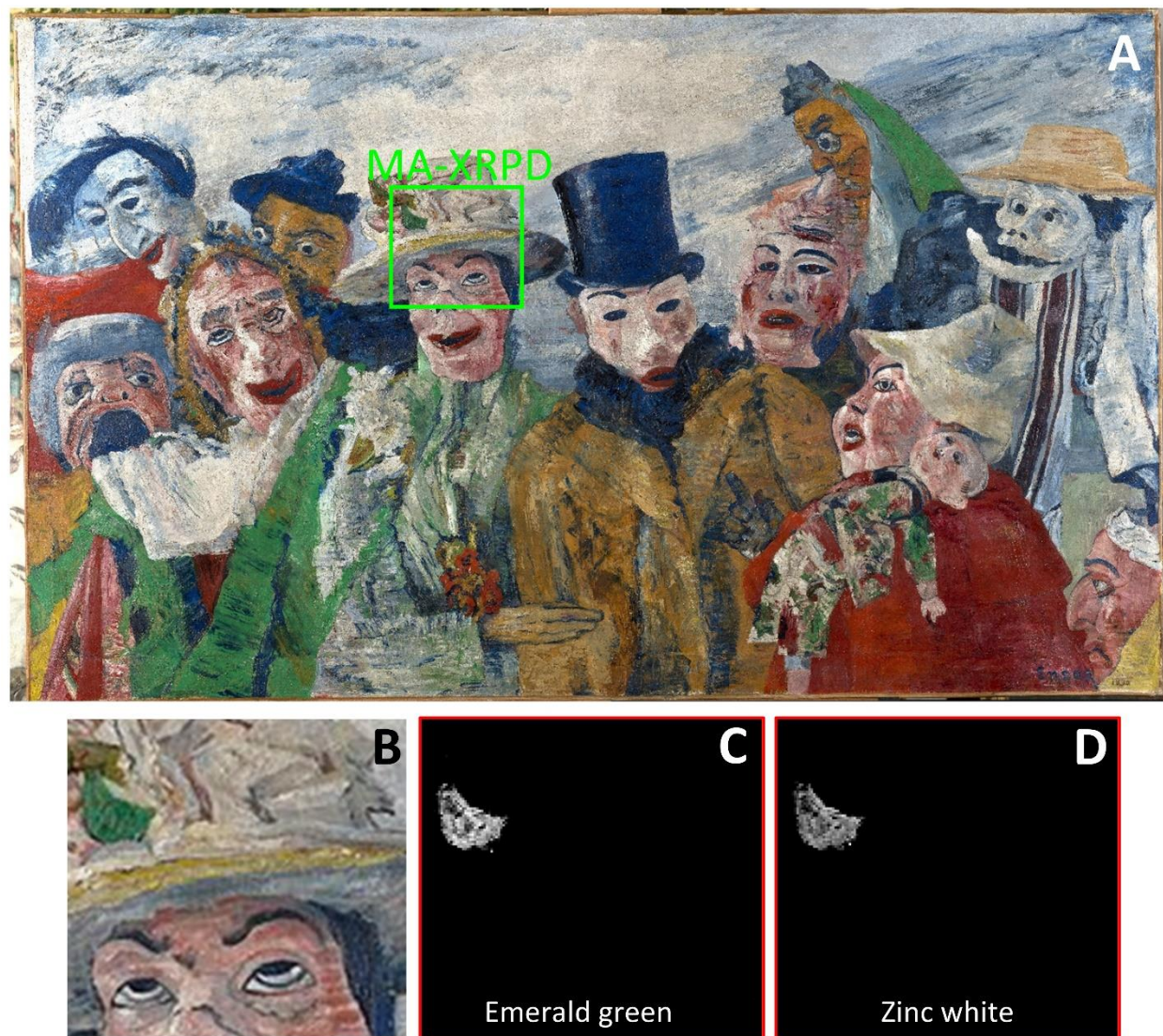


Fig. S1. MA-XRPD results of *The Intrigue* (1890). (A) Photograph of *The Intrigue* (1890) (Royal Museum of Fine Arts, Antwerp, Belgium; inventory number 1856) and area scanned via macro-X-ray diffraction (MA-XRPD) (green square). (B) Enlargement of the area scanned by MA-XRPD. Maps of crystalline phases identified in the green areas: (C) emerald green and (D) zinc white (ZnO) (map size (h×v):170×160 mm², step size: 1.2×1.2 mm², exposure time: 10 s/pixel).

Figure S2 shows the stratigraphic composition of microsamples M45 and M50 found with μ -XRPD analysis. In both samples, the green layers are made of a mixture of emerald green and zinc white (Fig. S2B,C,I,J). The ground yellow layer in M45 is primarily composed of a sulfate-rich chrome yellow type ($\text{PbCr}_{1-x}\text{S}_x\text{O}_4$, with $x \sim 0.5$) and lead white (in the form of hydrocerussite), with particles of ultramarine blue and vermilion (Fig. S2D-G).

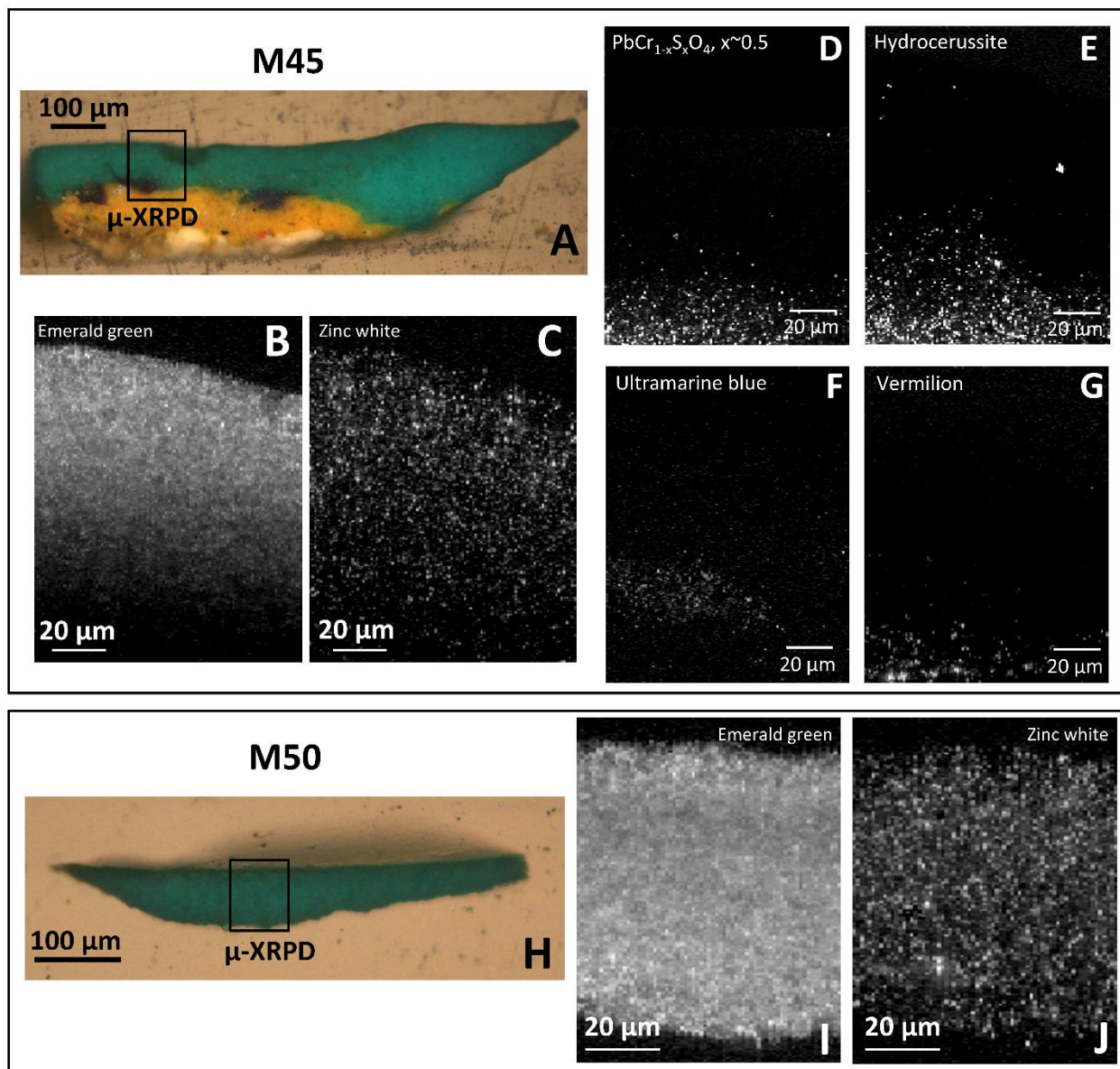


Fig. S2. μ -XRPD results from microsamples M45 and M50. Photomicrographs of the paint cross-sections (A) M45 and (H) M50 sampled from *The Intrigue* (see Fig. 1A for the sampling spots). Maps of crystalline phases identified in the green and yellow layers: (B,I) emerald green and (C,J) zinc white (ZnO), (D) sulfate-rich chrome yellow variety ($\text{PbCr}_{1-x}\text{S}_x\text{O}_4$, with $x \sim 0.5$), (E) lead white (hydrocerussite), (F) ultramarine blue and (G) vermilion, respectively for (B-G) M45 (map size ($h \times v$): $100 \times 130 \mu\text{m}^2$, step size ($h \times v$): $1 \times 0.5 \mu\text{m}^2$, dwell time: 0.3 s/pixel) and (I,J) M50 (map size ($h \times v$): $70 \times 110 \mu\text{m}^2$, step size: $1 \times 0.5 \mu\text{m}^2$, dwell time: 0.3 s/pixel).

S3. Linear combination fitting (LCF) results of As K-edge XANES spectra

Table S1. LCF results. Quantitative As speciation percentages obtained by LCF fitting of As K-edge μ -XANES spectra for cross-section M50, aged paint sections, and powder sample. Fit errors are reported.

Sample	Depth (μm)	Component weight (%)						Fit error		
		Emerald green	$\text{Cu}_2\text{AsO}_4(\text{OH})$	$\text{Ca}_3(\text{AsO}_4)_2$	As_2O_3	Approximated $[\text{As}^{3+}]/[\text{As}_{\text{tot}}]$	Approximated $[\text{As}^{5+}]/[\text{As}_{\text{tot}}]$	R-factor	Chi-square	Reduced chi-square
M50	0 (surface)	55 \pm 1	23 \pm 4	22 \pm 4	-	55	45	0.0056	0.1001	0.0011
	2.5	76 \pm 1	-	24 \pm 1	-	75	25	0.0025	0.0388	0.00041
	5	58 \pm 1	-	4 \pm 2	38 \pm 1	95	5	0.0010	0.0150	0.00016
EG _{paint tube-UVA-VIS}	0 (surface)	66 \pm 2	34 \pm 2	-	-	65	35	0.0150	0.3401	0.0037
	2.5	72 \pm 1	28 \pm 1	-	-	70	30	0.0020	0.0419	0.00044
	5	69 \pm 1	11 \pm 1	-	20 \pm 1	90	10	0.0018	0.0373	0.00039
	7.5	56 \pm 1	3 \pm 1	-	41 \pm 1	95	5	0.0027	0.0496	0.00052
	10	71 \pm 1	-	-	29 \pm 1	100	-	0.0017	0.0324	0.00034
	12.5	58 \pm 1	-	-	42 \pm 2	100	-	0.0055	0.0981	0.0010
	160	65 \pm 1	-	-	35 \pm 1	100	-	0.0030	0.0571	0.00061
EG _{synth-UVA-VIS}	0 (surface)	40 \pm 1	20 \pm 5	40 \pm 5	-	40	60	0.0135	0.2224	0.0024
	2.5	51 \pm 1	49 \pm 3	-	-	50	50	0.0105	0.1972	0.0022
	5	62 \pm 1	38 \pm 3	-	-	60	40	0.0147	0.2896	0.0031
	7.5	68 \pm 1	32 \pm 3	-	-	70	30	0.0091	0.1748	0.0019
	10	83 \pm 1	17 \pm 3	-	-	85	15	0.0050	0.0974	0.0010
	15	91 \pm 1	9 \pm 1	-	-	90	10	0.0076	0.1388	0.0015
EG _{comm-UVA-VIS}	0 (surface)	40 \pm 1	21 \pm 4	39 \pm 4	-	40	60	0.0079	0.1331	0.0014
	2.5	52 \pm 1	25 \pm 3	23 \pm 3	-	50	50	0.0033	0.0564	0.00061
	5	81 \pm 1	19 \pm 3	-	-	80	20	0.0029	0.0573	0.00063
	7.5	76 \pm 1	5 \pm 1	-	19 \pm 1	95	5	0.0033	0.0585	0.00064
EG* _{synth-UVA-VIS}	-	68 \pm 1	12 \pm 4	20 \pm 4	-	70	30	0.0074	0.1244	0.0015
EG _{synth-95%RH}	0 (surface)	25 \pm 6	-	11 \pm 2	64 \pm 4	90	10	0.0183	0.3482	0.0033
	2.5	91 \pm 1	-	-	9 \pm 1	100	-	0.0029	0.0590	0.00062
	97	78 \pm 1	-	6 \pm 1	16 \pm 1	95	5	0.0013	0.0321	0.00032

S4. Cu K-edge μ -XANES investigations of *The Intrigue* and photoaged mock-ups

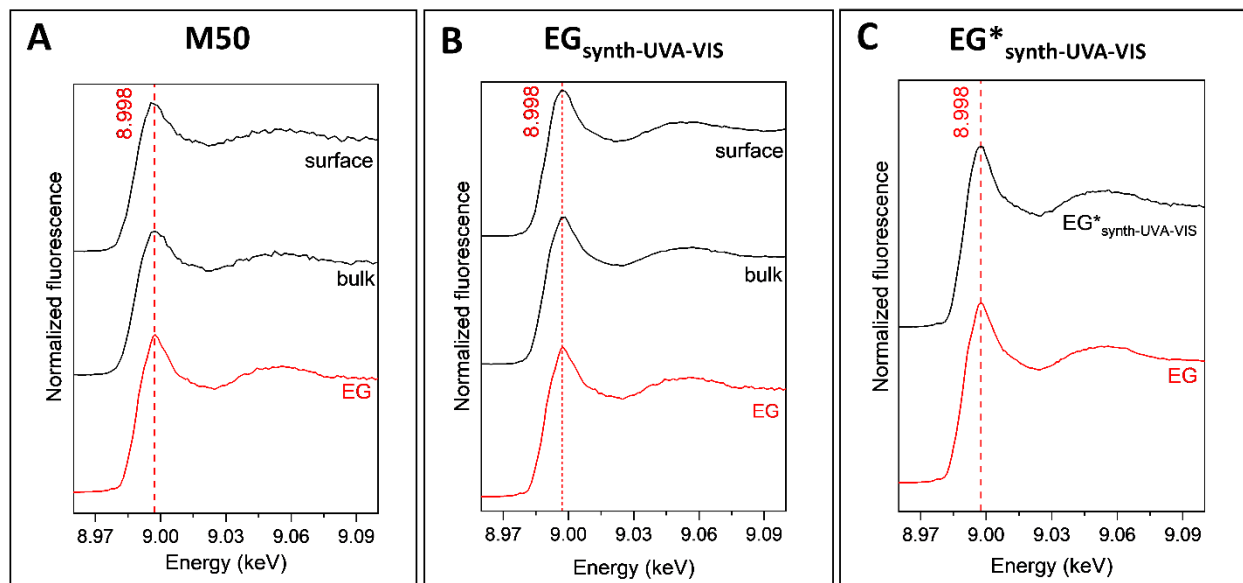


Fig. S3. Cu speciation results from microsample M50 and photoaged EG_{synth} paint and powder. Selected Cu K-edge μ -XANES spectra for (A) historical paint cross-section M50, (B) $EG_{\text{synth-UVA-VIS}}$ paint and (C) $EG^*_{\text{synth-UVA-VIS}}$ powder. The spectrum of emerald green is reported in red for comparison.

S5. Characterization of emerald green samples and unaged paint mock-ups

Table S2. XRPD characterization of powders and the paint tube. Summary of XRPD results for synthesized powder (EG_{synth}), commercial powder (EG_{comm}) and paint tube (EG_{paint tube}). Rietveld refinement was used to determine the refined unit cell parameters (a, b, c, β), microstrain (ϵ , expressed as percentage of the average unit cell deformations), the average crystallite size (Dv) and the phase weight percentage (wt (%)).

Sample	Phase	Crystal system	a (Å)	b (Å)	c (Å)	β (°)	ϵ (%)	Dv (μm)	wt (%)
EG _{synth}	EG	monoclinic	9.889(2)	9.366(1)	5.535(1)	101.80(1)	1.9	≥ 1	100
EG _{comm}	EG	monoclinic	9.914(3)	9.382(1)	5.524(1)	101.71(1)	1.5	0.4	-*
	CuAs ₂ O ₄	tetragonal	8.598(1)	8.598(1)	5.549(1)	-	0.5	0.2	-*
EG _{paint tube}	EG	monoclinic	9.964(2)	9.382(1)	5.521(1)	101.64(1)	1.1	0.1	98.4(1)
	As ₂ O ₃	cubic	11.049(1)	11.049(1)	11.049(1)	-	-†	0.1	1.6(1)

* XRPD patterns were acquired without any internal standard. The presence of a semicrystalline phase hindered an accurate quantification of emerald green and trippkeite.

† The wt% of arsenolite was too low to permit a reliable estimation of ϵ .

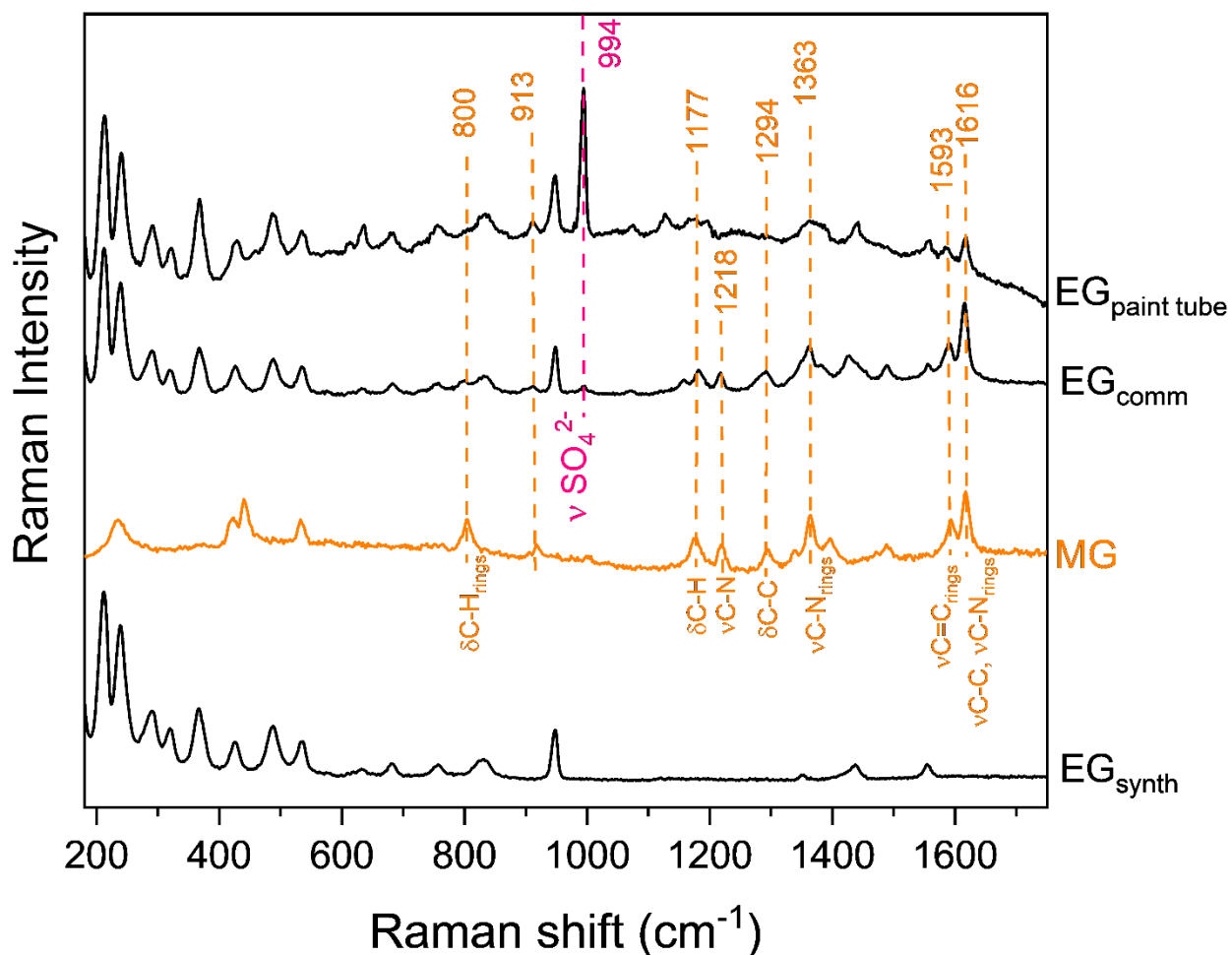


Fig. S4. μ -Raman characterization of powders and the paint tube. μ -Raman spectra of EG_{synth}, EG_{comm} and EG_{paint tube} (black) compared to that of malachite green dye (MG, 4-[(4-dimethylamminofenil)-fenil-metil]-N,N-dimetil-anilinio) (orange) (acquisition conditions: $\lambda=514.5$ nm, exposure time: 5 s, 5 accumulations).

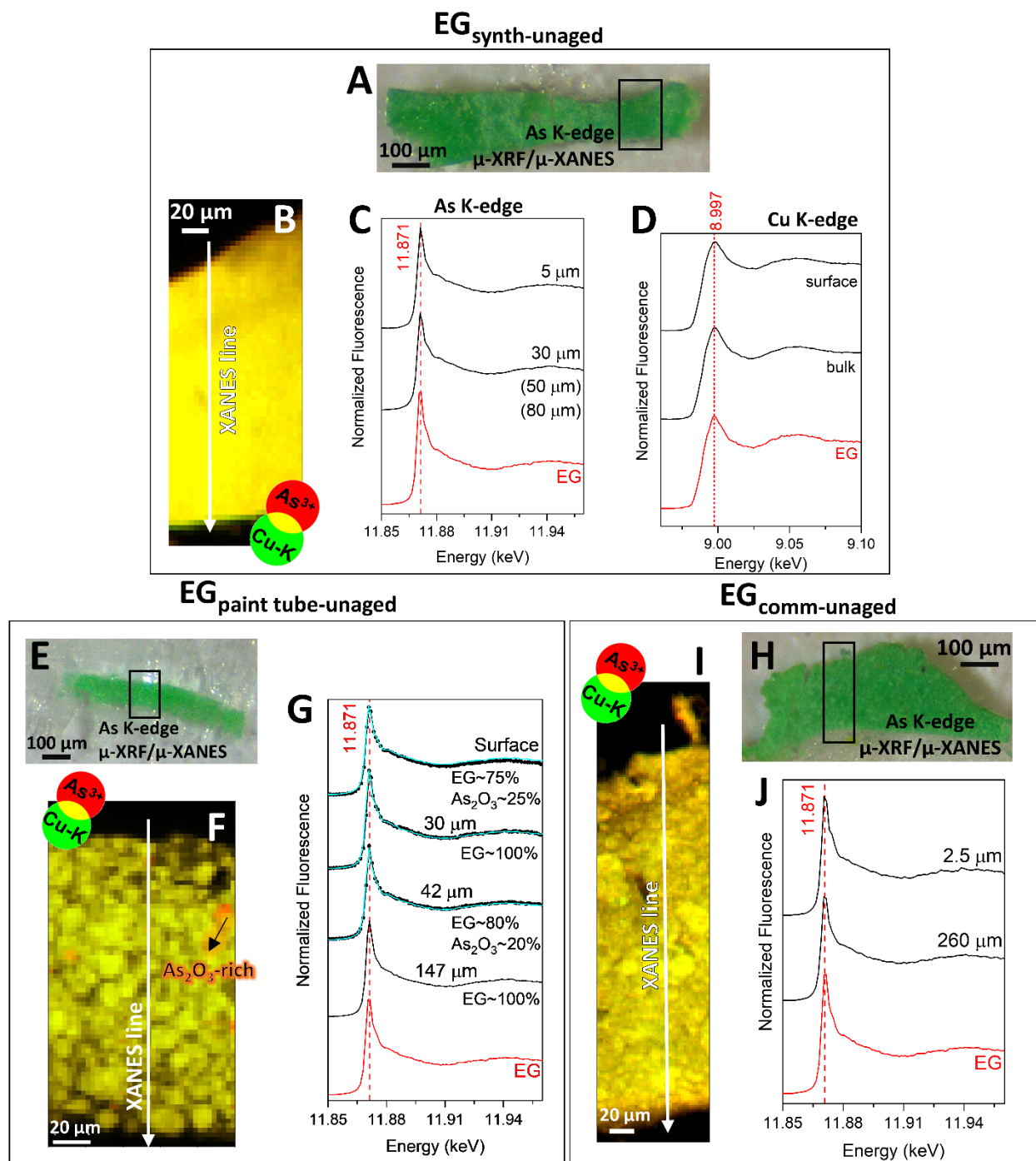


Fig. S5. As and Cu speciation results from unaged paint mock-ups. Photomicrograph of thin sections of unaged (A) EG_{synth}, (E) EG_{paint tube} and (H) EG_{comm} and corresponding (B,F,I) RG SR μ -XRF maps of As³⁺/Cu-K ((B) map size (h \times v): 80 \times 170 μ m², (F) map size (h \times v): 97.5 \times 520 μ m², (I) map size (h \times v): 100 \times 185 μ m², step size (h \times v): 2.5 \times 2.5 μ m², dwell times: 0.1-0.2 s/pixel). (C,G,J) Selected As K-edge μ -XANES spectra extracted from the XANES line shown in (B,F,I). Numbers in brackets indicate spectra with similar profiles to those plotted. In (G) the LCF results (cyan) of different As-based compounds to the XANES spectra are also shown. (D) Average Cu K-edge μ -XANES spectra obtained from three measurement points on the surface and in the bulk. The As K- and Cu K-edges μ -XANES spectra of emerald green (red) are shown for comparison.

S6. As and Cu speciation investigations and XRPD of photoaged mock-ups and powder

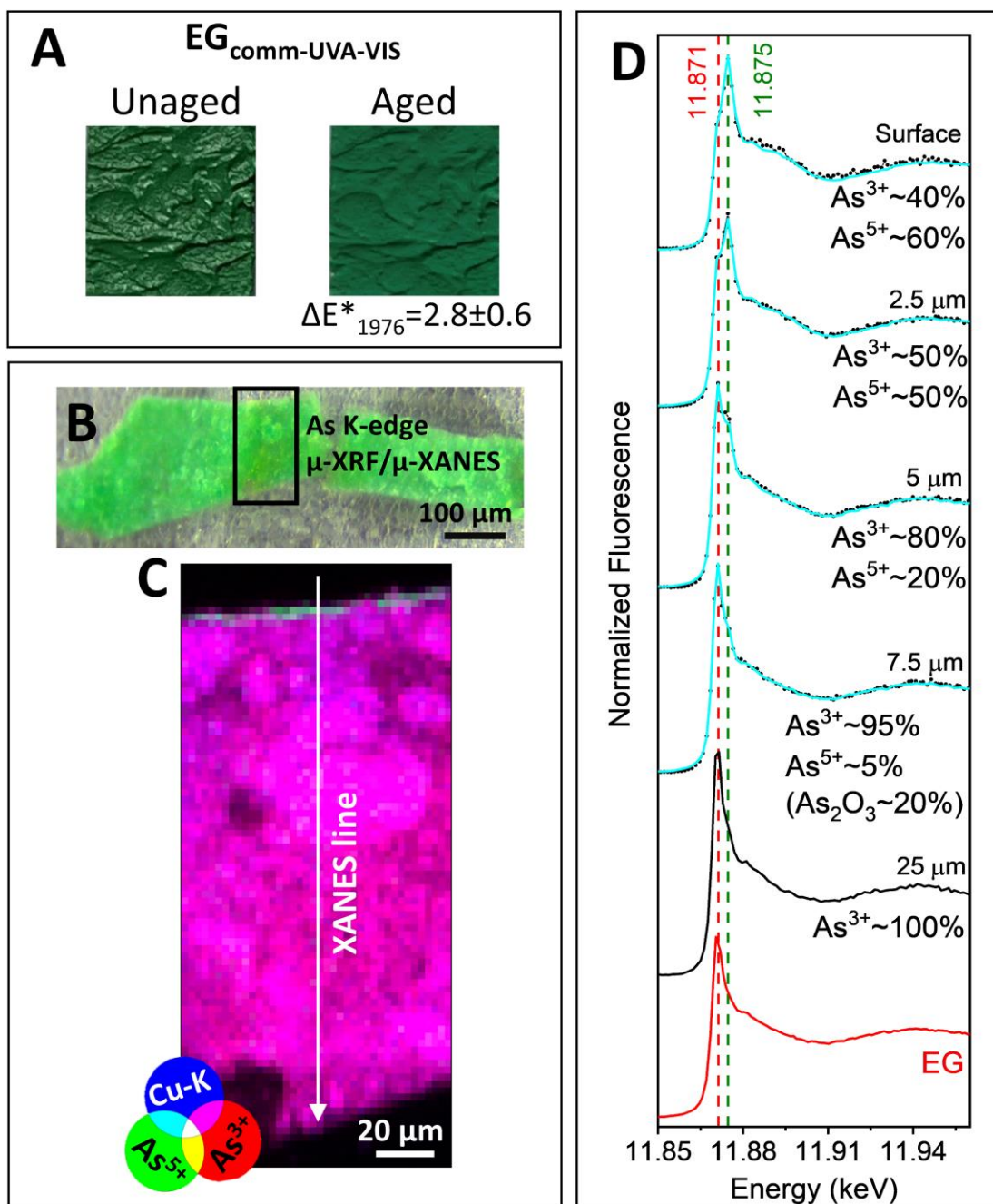


Fig. S6. Photochemically aged EG_{comm} paint mock-up. (A) Photographs of EG_{comm} oil paint mock-up before and after exposure to UVA-VIS light, showing the corresponding color variation (ΔE^*_{1976}). (B) Photomicrograph of the $EG_{\text{comm-UVA-VIS}}$ thin-section and relative (C) RGB SR $\mu\text{-XRF}$ maps of $As^{3+}/As^{5+}/Cu\text{-K}$ (map size (h×v): $100 \times 250 \mu\text{m}^2$, step size (h×v): $2.5 \times 2.5 \mu\text{m}^2$, dwell time: 0.2 s/pixel). (D) Selected As K-edge $\mu\text{-XANES}$ spectra acquired from the $EG_{\text{comm-UVA-VIS}}$ paint along the line shown in (C), with corresponding LCF results (cyan) for different As-based compounds. The spectrum of emerald green is shown in red for comparison.

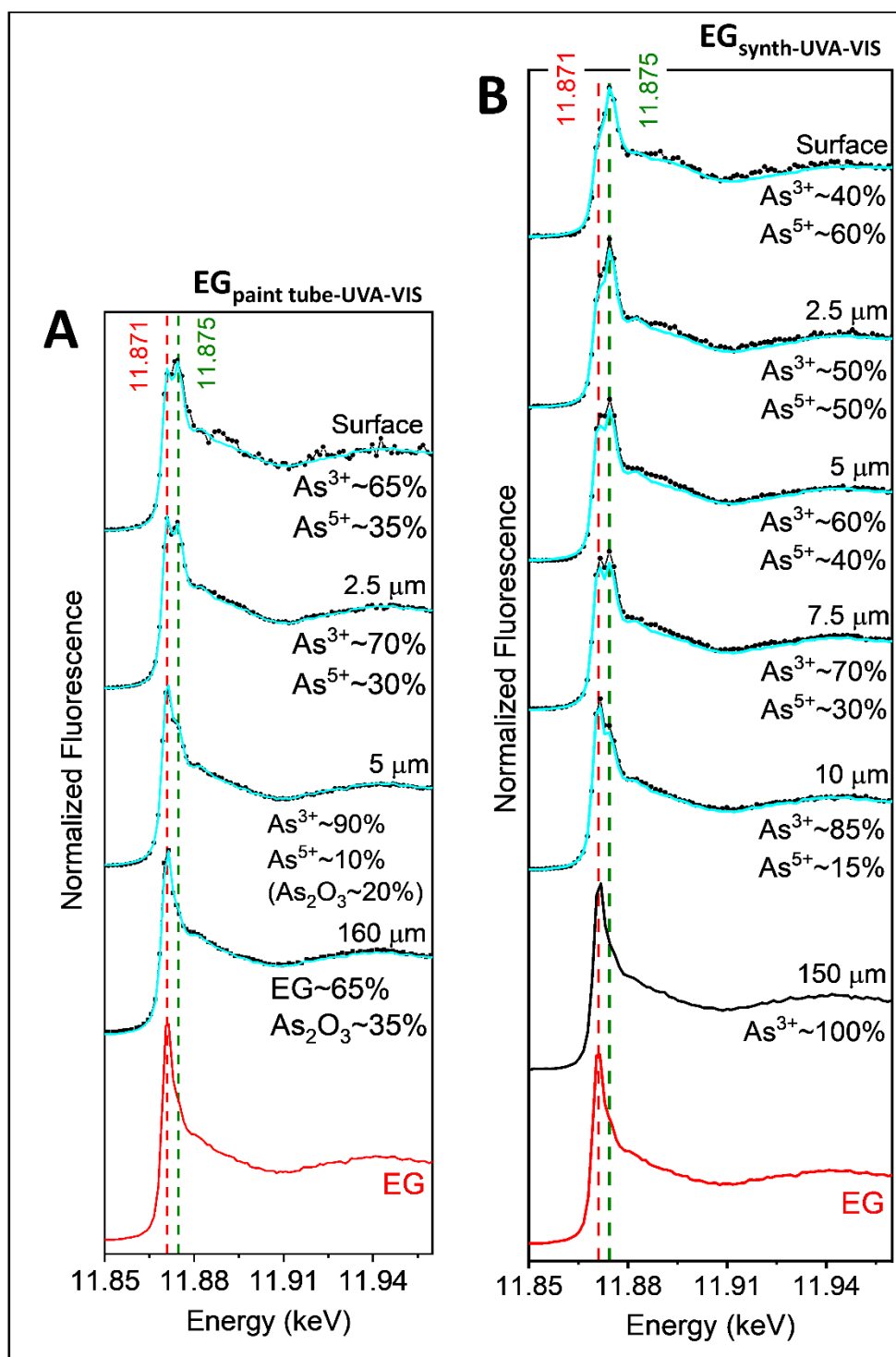


Fig. S7. Photoaged $EG_{\text{paint tube}}$ and EG_{synth} mock-ups: As K-edge XANES results. Selection of As K-edge μ -XANES spectra acquired from (A) $EG_{\text{paint tube-UVA-VIS}}$ and (B) $EG_{\text{synth-UVA-VIS}}$ paints along the line shown in Figure 4D,F and corresponding LCF results (cyan) of different As-based compounds. The spectrum of emerald green is reported in red for comparison.

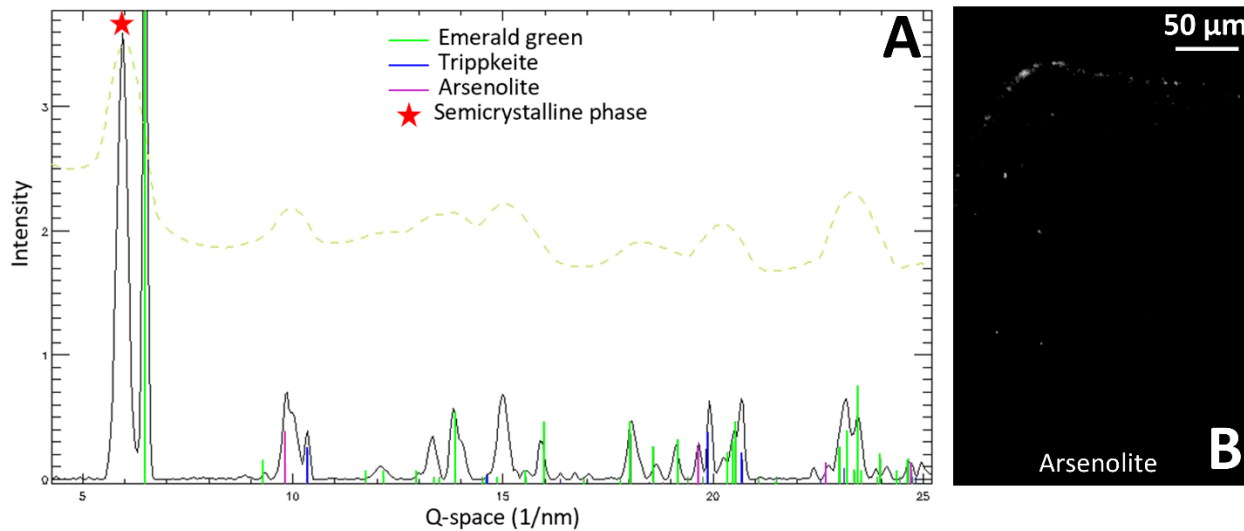


Fig. S8. Photoaged EG_{comm} mock-up: μ-XRPD results. (A) SR μ-XRPD average pattern from the surface of EG_{comm-UVA-VIS} thin section. (B) SR μ-XRPD map of arsenolite (As₂O₃) (map size (h×v): 235×380 μm², step size (h×v): 1×1 μm², dwell time: 0.02 s/pixel, energy: 12.92 keV).

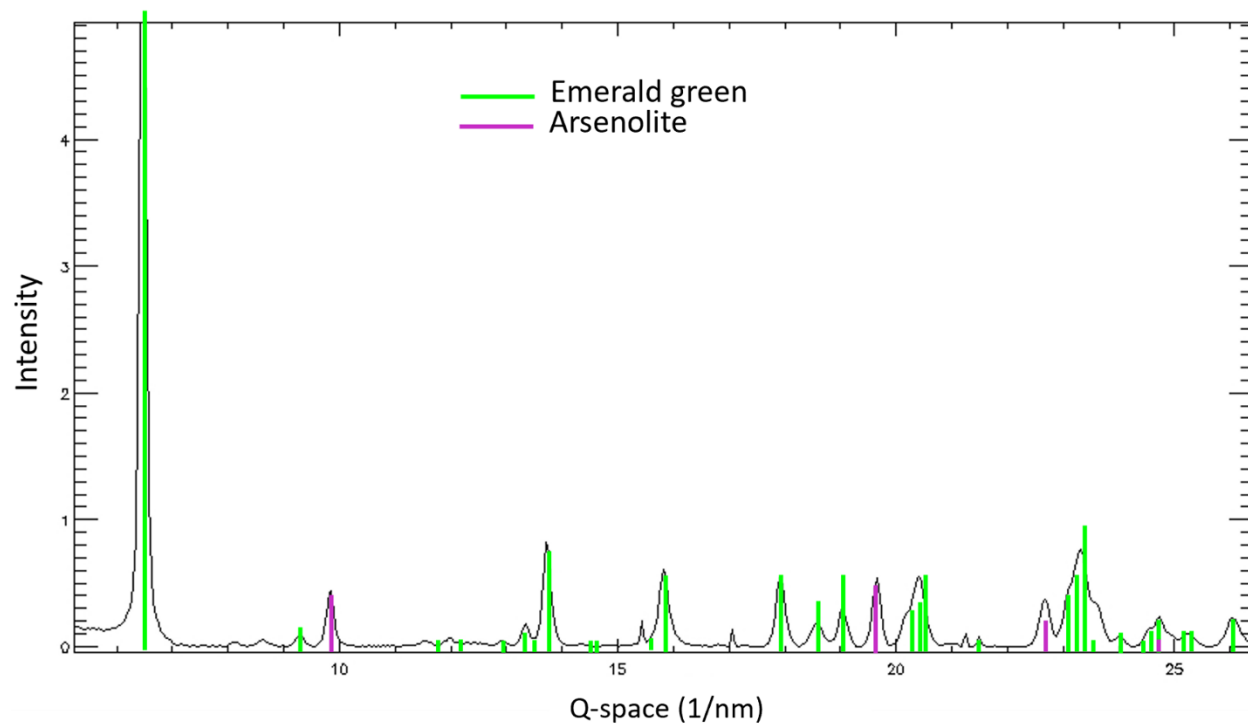


Fig. S9. Photoaged EG*_{synth} powder: μ -XRPD results. SR μ -XRPD average pattern from the EG*_{synth}-UVA-VIS powder analyzed (map size (h \times v): 80 \times 90 μm^2 , step size (h \times v): 0.5 \times 10.5 μm^2 , dwell time: 0.2 s/pixel).

S7. Assessment of synchrotron radiation-based X-ray induced damage

To preserve sample integrity and prevent misinterpretation of data, we performed a series of X-ray radiation damage tests on unaged synthesized emerald green paint, monitoring them using As and Cu K-edge XANES measurements.

We acquired three consecutive As K-edge μ -XANES spectra on the same spot under environmental conditions. Fluence values were varied: “low fluence” (ca. $7.5 \cdot 10^{10}$ ph/ μm^2), “high fluence” (ca. $4 \cdot 10^{11}$ ph/ μm^2), and again “low fluence” (ca. $7.5 \cdot 10^{10}$ ph/ μm^2), progressively increasing the total fluence at the same spot. Under all these experimental conditions, no significant changes in the arsenic oxidation state were observed, confirming it remained as As^{3+} (Fig. S10A). Based on these results, we decided to perform measurements using “low fluence” conditions.

For measurements at Cu K-edge, we carried out a first radiation damage test by recording a sequence of ten μ -XANES spectra in the vacuum at the same point of $\text{EG}_{\text{synth-unaged}}$ sample. Spectra were acquired by scanning the primary energy of the incident beam across the Cu K-edge, from 8.95 to 9.3 keV, with an increment of 0.5 eV and 0.1 s/pt. Attenuators reduced the flux to ca. 10^{10} ph/s, resulting in a total fluence of ca. $4 \cdot 10^{12}$ ph/ μm^2 for one scan. These conditions were defined as “high fluence”. A pre-edge shoulder, appearing at around 8.981-8.983 keV and possibly related to Cu^+ compounds, appeared after just one scan, with its intensity increasing proportionally to the total fluence (Fig. S10B). Therefore, softer experimental conditions were chosen for a second radiation damage test on a different spot of the paint: (i) reduced acquisition spectral range (from 8.95-9.3 keV to 8.98-9.2 keV); (ii) increased energy step (from 0.5 eV to 1 eV); (iii) lowered flux from ca. 10^{10} ph/s to $8 \cdot 10^9$ ph/s obtained using a second attenuator and resulting in a fluence of ca. $1 \cdot 10^{12}$ ph/ μm^2 (defined as “low fluence”). These newly selected experimental conditions significantly reduced the probability of formation of Cu^+ compounds due to X-ray beam exposure (Fig. S10C).

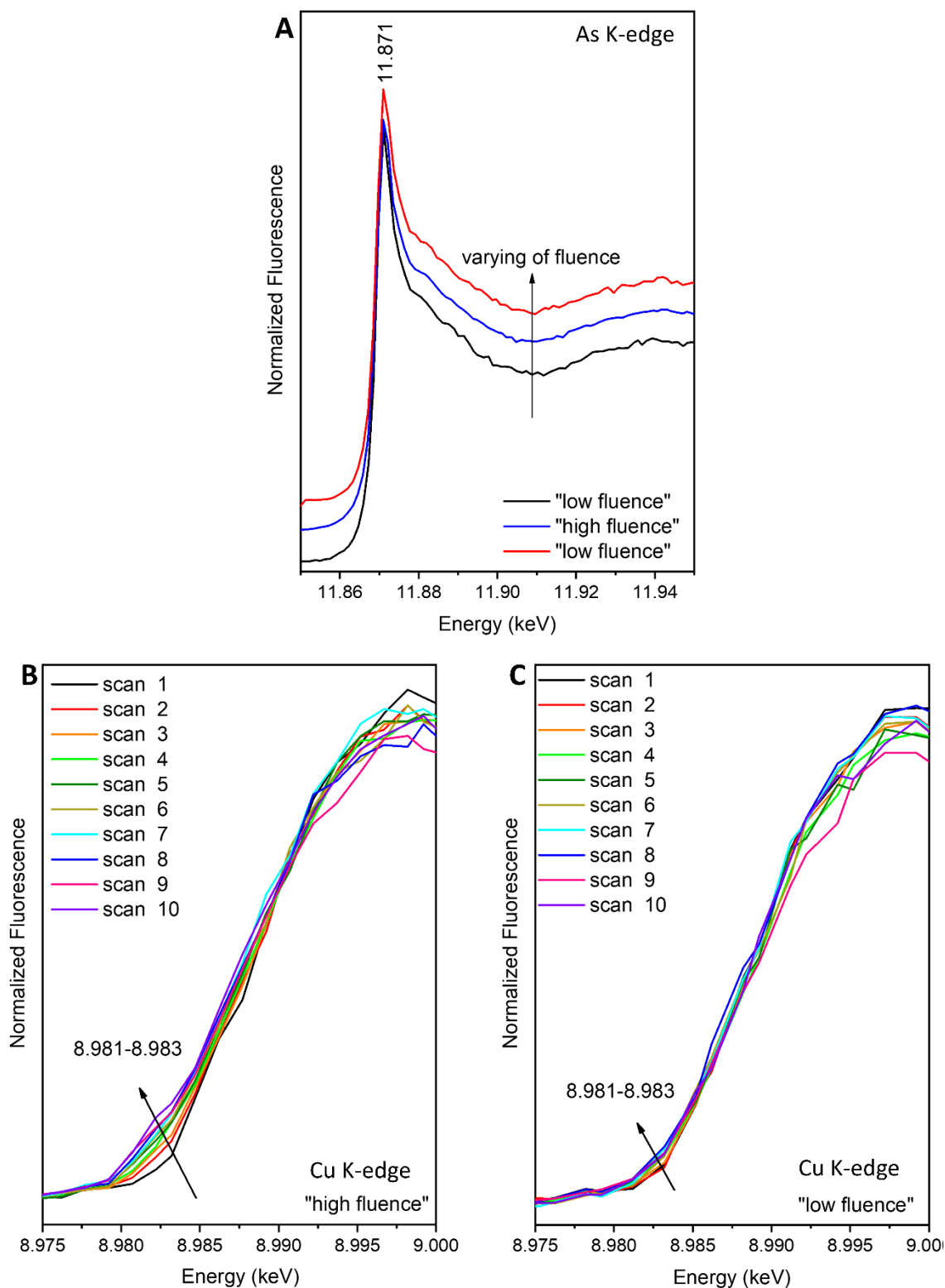


Fig. S10. SR-based X-ray induced damage. (A) As-K edge μ -XANES spectra acquired from EG_{synth-unaged} at the same spot, varying the fluence values from ca. $7.5 \cdot 10^{10}$ ph/ μm^2 ("low fluence"), to ca. $4 \cdot 10^{11}$ ph/ μm^2 ("high fluence"). Sequence of n. 10 Cu K-edge μ -XANES spectra acquired at the same spot of the paint EG_{synth-unaged} with (B) ca. $4 \cdot 10^{13}$ ph/ μm^2 ("high fluence") and (C) ca. $1 \cdot 10^{13}$ ph/ μm^2 ("low fluence").